Journal of Hazardous Materials 162 (2009) 1211–1216

Contents lists available at ScienceDirect

Journal of Hazardous Materials

journal homepage: www.elsevier.com/locate/jhazmat

Identification of produced powerful radicals involved in the mineralization of bisphenol A using a novel UV-$Na_2S_2O_8$/H_2O_2-Fe(II,III) two-stage oxidation process

Yi-Fong Huang[a], Yao-Hui Huang[a,b,*]

[a] Department of Chemical Engineering, National Cheng Kung University, Tainan City 701, Taiwan
[b] Sustainable Environment Research Center, National Cheng Kung University, Tainan City 701, Taiwan

ARTICLE INFO

Article history:
Received 11 April 2008
Received in revised form 4 June 2008
Accepted 4 June 2008
Available online 8 June 2008

Keywords:
Endocrine disrupting chemicals
Bisphenol A
Persulfate
Photo-Fenton
Mineralization

ABSTRACT

A two-stage oxidation (UV-$Na_2S_2O_8$/H_2O_2-Fe(II,III)) process was applied to mineralize bisphenol A (BPA) at pH_i (initial pH) 7. We take advantage of the high oxidation potential of sulfate radicals and use persulfate as the 1st-stage oxidant to oxidize BPA to less complex compounds (stoichiometric ratio: $[S_2O_8^{2-}]_0/[BPA]_0 = 1$). Afterwards, the traditional photo-Fenton process was used to mineralize those compounds to CO_2. To the best of our knowledge, this is the first attempt to utilize the two processes in conjunction for the complete degradation of BPA. During the 2nd-stage reaction, other oxidants (H_2O_2 and Iron alone) were also employed to observe the extent of enhancement of photo-Fenton. Further, qualitative identification of both hydroxyl and sulfate radicals was performed to evaluate their dominance under different conditions. The BPA degradation in this UV/persulfate process formulated a pseudo-first-order kinetic model well, with a rate constant of approximately 0.038 min^{-1} (25 °C), 0.057 min^{-1} (35 °C), and 0.087 min^{-1} (50 °C), respectively. The much lower activation energy ($\Delta E = 26$ kJ mol^{-1}) was further calculated to clarify that the thermal-effect of an illuminated system differs from single heat-assisted systems described in other research. Final total organic carbon (TOC) removal levels of BPA by the use of such two-stage oxidation processes were 25–34%, 25%, and 87–91% for additional Fe(II,III) activation, H_2O_2 promotion, and Fe(II,III)/H_2O_2 promotions, respectively.

1. Introduction

Bisphenol A [BPA: 2,2-bis(4-hydroxyphenyl)propane] was first manufactured by ALBERT Company in Germany in 1923. The vast majority of it, greater than 99.9%, is consumed at manufacturing sites to make products such as synthesized polymers including polycarbonates, epoxy resins, phenol resins, polyesters, and polyacrylates [1]. BPA dust (particulate) is controlled by workplace practices and engineering design and is not a significant contributor to environmental pollution. The relatively small amount of vapor released into the atmosphere can be rapidly degraded by sunlight. However, low levels (ppb to ppm levels) of BPA was released into effluent water, and even after biological wastewater treatment, the residuals still remain harmful to the environment and human health [2].

Recently, biphenolic compounds including BPA have been recognized as endocrine disrupting chemicals (EDCs) [3]. Unfortunately, the presence of these compounds in effluents at low but environmentally relevant levels, indicates that traditional technologies are not sufficiently effective for treating these compounds. Thus, it is not only necessary to assess the biodegradability or fate of BPA in the natural environment, but also lower its toxicity. New biodegradation technologies are under development to target such compounds for treatments, including enzymatic processes [4,5], but the common drawbacks of biodegradation technologies, such as a long reaction time required (several days to months), still remain. Even the powerful advanced oxidation processes such as Fenton's reaction (Eq. (1)) is limited by low pH conditions ($pH_i < 4$) [6].

$$Fe^{2+} + H_2O_2 \rightarrow Fe^{3+} + OH^- + {}^{\bullet}OH, \qquad k = 63\ M^{-1}\ S^{-1} \tag{1}$$

However, some researchers recently have improved this drawback in the presence of ligands to iron, pH can be expanded to neutral region [7,8].

Another oxidation method was proposed based on the high redox potential ($E_0 = 2.01$ V) of persulfate ($S_2O_8^{2-}$), which is used

* Corresponding author at: Department of Chemical Engineering, National Cheng Kung University, Tainan City 701, Taiwan. Tel.: +886 6 2757575x62636; fax: +886 6 2344496.
E-mail address: yhhuang@mail.ncku.edu.tw (Y.-H. Huang).

0304-3894/$ – see front matter © 2008 Elsevier B.V. All rights reserved.
doi:10.1016/j.jhazmat.2008.06.008

less frequently than ozone ($E_0 = 2.07$ V) [9]. Persulfates are used as initiators in the emulsion polymerization processes, detergents, bleaching agents, and in the etching of Cu-printed circuit boards. Recently, persulfate was commercially used in a total organic carbon (TOC) analyzer as an oxidant and has additionally been used for in-situ chemical oxidation (ISCO) of contaminated soil and groundwater.

The decomposition of persulfate in aqueous solution is an important step to yield sulfate radicals ($SO_4^{-\bullet}$, $E_0 = 2.60$ V) for strong oxidation [10,11], and such radicals can also react with water to yield hydroxyl radicals [12,13]:

$$SO_4^{-\bullet} + H_2O \rightarrow H^+ + SO_4^{2-} + {}^{\bullet}OH \quad (2)$$

Although, the reaction rate constant is very low ($k < 60\ M^{-1}\ s^{-1}$), such that the reaction is not a major sink for sulfate radicals; the $SO_4^{-\bullet}$ radical, however, has high efficacy on organic matter.

We take advantage of the high oxidation–reduction potential of sulfate radicals and use persulfate as the 1st-stage oxidant to oxidize BPA to less complex compounds (stoichiometric ratio: $[S_2O_8^{2-}]_0/[BPA]_0 = 1$). Afterwards, the traditional photo-Fenton process was then used to mineralize those compounds to CO_2 or to decompose it to be biodegradable. To the best of our knowledge, this is the first attempt to utilize the uniqueness of the two processes for the complete degradation (mineralization) of BPA, instead of utilizing a single persulfate oxidation process with a high stoichiometric ratio of persulfate [11,14,15]. During the 2nd-stage reaction, other oxidants (H_2O_2 and iron alone) were also employed to observe the extent of enhancement of photo-Fenton [6,7]. Further, the qualitative identification of both hydroxyl and sulfate radicals was performed to evaluate their dominance under different conditions.

Consequently, this study was undertaken to overcome the common disadvantages of traditional methods, thus developing a novel technology we call "UV-$Na_2S_2O_8$/H_2O_2-Fe(II,III) two-stage oxidation process". BPA was chosen as the model EDC contaminant, and a high TOC removal, related to complete mineralization, was expected to be achieved in order to destroy its toxicity. A significant benefit from this concept is to directly practice the treatment of BPA, even in alkaline conditions ($pH_i \geq 7$), no matter whether the case is ISCO, or not. The powerful oxidants will serve as identified $SO_4^{-\bullet}$ and ${}^{\bullet}OH$ radicals, which can be introduced coexistently to participate in the BPA decomposition reaction. Furthermore, a kinetic approach to persulfate participation in the BPA decomposition is also expected to be carried out.

2. Experimental

2.1. Materials

Bisphenol A was purchased from Showa. For reference, the chemical structure of BPA consists of two phenolic rings joined together through a bridging carbon which is displayed as the target EDC used in all trials. Sodium persulfate (SPS) was purchased from Riedel-de-Haën. Hydrogen peroxide (35 wt.%) solution was obtained from Nihon Shiyaku Reagent (Japan). Ferric sulfate and ferrous sulfate were purchased from Acros and Merck Chemical companies. 5,5-dimethyl-1-pyrroline-*N*-oxide (DMPO) was purchased from Sigma. Other chemicals used herein, including sulfuric acid and sodium hydroxide, were of reagent grade and were used to adjust pH. All sample solutions were prepared using deionized water from the Millipore Milli-Q system.

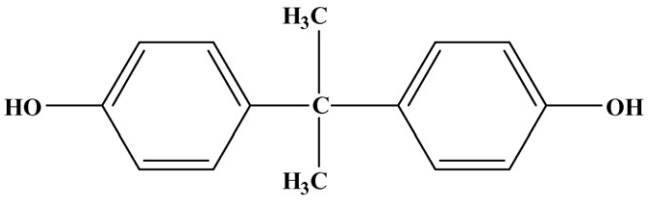

Chemical structure of Bisphenol A (BPA)

2.2. Experimental procedures and analysis

The photo-activation of the BPA degradation reactions in a batch photoreactor (Fig. 1) at reaction temperature was practiced. The irradiation source was a 15 W UV lamp (allowing mainly a wavelength $\lambda = 254$ nm to emit) fixed inside a cylindrical photoreactor, and the characteristics of the relative intensities of the emission wavelengths are shown in Fig. 2. After turning on the UV light and reaching a stable emission, 0.05 mM ($\sim$10 mg L^{-1}) BPA solution was adjusted to pH_i 7, while the estimated $Na_2S_2O_8$ (0.05 mM) was simultaneously added to the photoreactor in a thermostatic water bath to initiate the reaction. The H_2O_2 and/or iron catalyst (Fe(II) or Fe(III)) was then added to the reaction solutions as the beginning of the 2nd-stage oxidation process. The volume of all reactive solutions was 1.0 L in each trial. The optimal amount of $\sim$0.16 mM H_2O_2 (based on the theoretical oxygen demand (ThOD) of $[BPA]_i = 0.05$ mM) as oxidant and 0.045 mM Fe(II,III) ($\ll$the stoichoimetric ratio of $[Fe(II,III)]_i/[H_2O_2]_i = 1$) as extra activator was estimated, and then supplied to the system at the 2nd-stage of the reaction process.

As unfavorable halogen ions such as Cl^- participate in the reaction, they will simultaneously scavenge most of the radi-

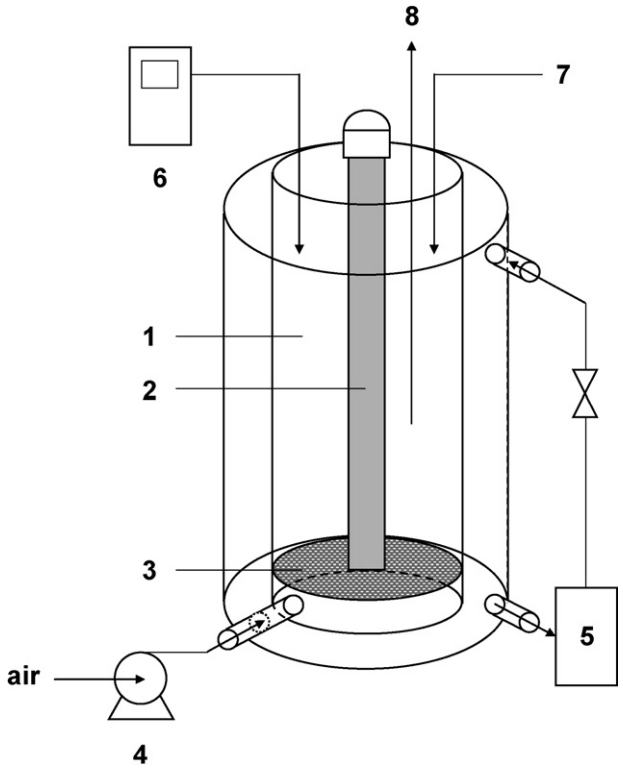

Fig. 1. Experimental equipment: (1) photoreactor, (2) UV lamp, (3) porous glass-plate, (4) air pump, (5) thermostat, (6) thermometer and pH meter, (7) feeding ($Na_2S_2O_8$ or H_2O_2 or Fe(II,III)) and (8) sampling.

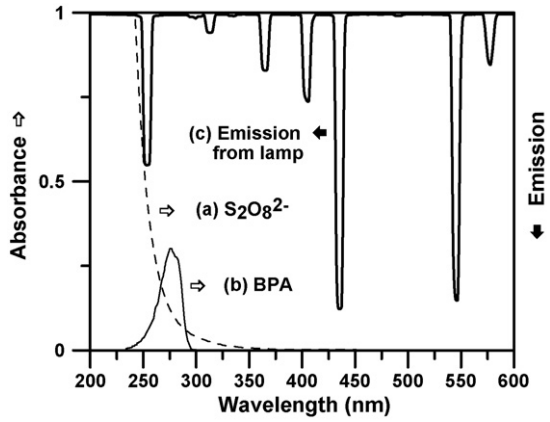

Fig. 2. Wavelength distribution for absorption of $S_2O_8^{2-}$ (10 mM in water) (b); BPA (0.1 mM in water) (c) and emission from the applied UV lamp (a). The path length for measurement of the absorption spectra was 1.0 cm set in a dynamic-UV analyser.

cals produced, thus generating chloride that may further transfer to Cl_2(g) as a result of the combination of two chloride atoms [13,16]. Due to the study requirement to clarify the kinetics of the BPA/$S_2O_8^{2-}$ oxidation system, all the reagents, including an acid source for pH adjusting and a Fe(II,III) source required for activation, are frequently used in the sulfate form instead of the chloride form to avoid such unwanted scavengers.

The residual H_2O_2 level was measured using titanium sulfate method [17]. TOC was measured using a TOC analyzer (Sievers 900 Portable). The performance of SO_4^{-} produced was detected using ion-exclusion chromatography with a 4.6 mm ID × 250 mm L Metrosep A SUPP 1 column (Metrohm, USA), which was not interfered with by the residual oxidants (H_2O_2 or $S_2O_8^{2-}$) during the reaction period.

An electron paramagnetic resonance (EPR) spectrometer from Bruker (model EMX-10; X-Band; 9 GHz) was used to detect whether the free radicals (SO_4^{-}• and/or •OH) were produced during the activation of persulfate with the degradation of BPA. DMPO (~0.07 M) was used as the radical spin-trapping reagent, while the EPR was operated on the following conditions: the center field = 3483 G, the sweep width = 100 G, the microwave frequency = 9.8 GHz, and the power setting = 400 W. The residual BPA level was measured after 0.5 mL methanol was added to each sample (1 mL) to quenched the radicals and thus terminate the reaction. The maximum absorption of BPA is at λ_{max} = 276 nm, and the removal of BPA were determined using high-performance liquid chromatography (Shimadzu 6A) with a TSK-GEL ODS-100S column (4.6 mm × 250 mm). Almost no Fe^{2+} ion residuals can be determined using the 1,10-phenanthroline method [18] during the degradation of BPA, in all of the 2nd oxidation processes. The Fe(II)-phenanthroline complex was evaluated spectrophotometrically at λ_{max} = 510 nm. All samples were analyzed immediately after sampling to prevent further reactions.

3. Results and discussion

3.1. Photo activation and radicals identification

When activated by heat or a UV source (254 nm), $S_2O_8^{2-}$ will decompose into two anionic free radicals (SO_4^{-}•) which are thought to be responsible for the degradation of BPA rather than the $S_2O_8^{2-}$ anion itself (Eq. (3)).

$$S_2O_8^{2-} \xrightarrow{h\nu/\Delta} 2SO_4^{-}\bullet \quad (3)$$

Fig. 2 shows the relationship between the wavelength distribution for absorption of $S_2O_8^{2-}$ and the emission from the UV lamp we used. As observed under suitable conditions, the lamp emits mainly 220–580 nm light. BPA absorbs sharply from 250 nm to 300 nm (λ_{max} = 276 nm) mainly and has weak, broad absorption to ~225 nm, whereas $S_2O_8^{2-}$ absorbs from the deep-UV region (<200 nm) to ~350 nm. Thus, $S_2O_8^{2-}$ was thought to be the dominant absorbing species in our study conditions [19]. It follows that this figure can also clarify that the predominant wavelength (λ = 254 nm) of the UV lamp we used was rarely directly responsible for the decomposition of the BPA, corresponding to the verified background data of curve (h) in Fig. 4.

The identification of SO_4^{-}• radicals was carried out by EPR, which has been mainly used for detection of radical species involved in polymerization, degradation and oxidation. The presence of unpaired electrons is a prerequisite for obtaining an EPR spectrum. Yet, when radical species are at a too low concentration or have a too short lifetime (~300 μs) for EPR detection [20], they should be converted further to yield an EPR detectable product, called a spin-adduct, by reaction with a spin-trapping agent. For this reason, a spin-trapping agent, DMPO, was used in this study to react with any radicals present in the reaction system [21]. After treatment with DMPO at 25 °C, the EPR spectra of SPS (pH < 4), alkali + SPS (pH > 11), photon + SPS (pH < 4), and alkali + photon + SPS (pH > 11) are shown in Fig. 3(a–d), respectively. Comparing the spectrum of Fig. 3(a and b) with Fig. 3(c and d), the characteristic peak of the •OH radical is much more obvious than that of the SO_4^{-}• radical in Fig. 3(c and d) due to the further transformation of SO_4^{-} to OH (Eq. (2)), and the side reaction (Eq. (4)) by the participation of the UV source as an efficient activator of persulfate photolysis.

$$SO_4^{-} + H_2O \xrightarrow{h\nu} SO_4^{2-} + \bullet OH + H^+ \quad (4)$$

The •OH spectrum and SO_4^{-}• spectrum are simultaneously identified from the intensity ratio of each characteristic peak as 1:2:2:1 [22] and 1:1:1 [21], respectively. The •OH spectrum is identified as the intensity ratio of 1:2:2:1 of the four symmetrical characteristic peaks, it is indicated by the series of symbols as ①:②:②:① in Fig. 3. Likewise, the SO_4^{-}• spectrum is identified as

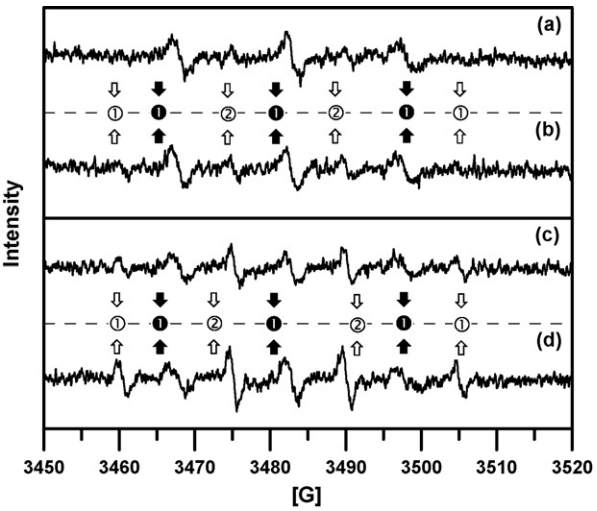

Fig. 3. EPR spetra of SPS (pH_i < 4) (a), alkali + SPS (pH_i > 10) (b), photon + SPS (pH_i < 4) (c), and alkali + photon + SPS (pH_i > 10) (d). Each trial of 0.05 mM SPS solution (acidic or alkaline) was, or was not, photo-activated within 1–2 min of illumination, and was thus detected by EPR with the participation of BPA to identify the expected SO_4^{-}• and •OH produced. Center field = 3483 G, sweep width = 100 G, microwave frequency = 9.8 GHz, and power setting = 400 W and operating temperature = 25 °C.

the intensity ratio of 1:1:1 of the three symmetrical characteristic peaks, it is also indicated by the series of symbols as ❶:❶:❶ in Fig. 3. From this point of view, $SO_4^{-\bullet}$ starts to decompose and transform into •OH rapidly as the solution pH > 8.5, and, furthermore, •OH will become the dominator when the solution pH > 10.7 [20]. On the contrary, $SO_4^{-\bullet}$ is rather stable in acidic solutions.

This concept is directly proved in Fig. 3. In comparison, the reaction pH of Fig. 3(a and c) is acidic, but the pH of Fig. 3(b and d) is greater than 11 so that the •OH spectrum is more obvious than that in Fig. 3(a and c), respectively. Contrarily, the $SO_4^{-\bullet}$ spectrum of Fig. 3(a and c) is more obvious than in Fig. 3(b and d), respectively. It seems even more likely that only the $SO_4^{-\bullet}$ spectrum could be observed in Fig. 3(a) due to the very low concentration (0.05 mM) of SPS required to conform to the conditions of each trial. This result also indicated that such a small dosage of oxidant ($[SPS]_0/[BPA]_0 = 1$) is sufficient to produce $SO_4^{-\bullet}$ radicals which can be detected from EPR treatment (with DMPO) after few minutes (~6 min), directly verifying that these expected strong radicals ($SO_4^{-\bullet}$ and •OH) are both present to further oxidize BPA.

3.2. Matel activation and H_2O_2 promotion

Goulden and Anthony [23] found that under strong acidic conditions (pH 1.2), the removal rate of nicotinic acid (target contaminant) is greater than it in alkaline conditions (pH 12), but worse than at pH 5. Thus, solutions with extreme acidic or basic conditions are unfavorable for persulfate oxidation.

When the decomposition of persulfate is carried out in unbuffered solutions, the pH will drop as the reaction proceeds. If it falls low enough, an increase in the rate of decomposition due to a significant contribution from the acid-catalyzed pathway will become important. Under alkaline conditions, the decomposition rate is lower than under acidic conditions, and the reversible reaction is also insignificant. However, when pH > 14, the decomposition rate will increase and OH-catalyzed reactions become important [14,20,24,25].

Therefore, all the experimental trials in our systems were practiced at pH_i 7 due to a large application range (pH 1.2–12) of persulfate to break the limitations of Fenton's reagent ($pH_i < 4$). In such un-buffered systems, solution pH will drop to pH < 4 to conform to $S_2O_8^{2-}$ decomposition as the reaction proceeds, thus it will contribute to the utilization of extra Fe(II,III) ions in the 2nd-stage of oxidation of BPA.

The sulfate radicals are stable in neutral and acidic solutions, but they will apparently be converted to hydroxyl radicals in the presence of oxygen at a pH > 8.5, and they completely disappear at pH 10.7–10.8 [20]. This implies that not only $SO_4^{-\bullet}$, but also •OH participates in the oxidation of BPA. At pH_i 7, $SO_4^{-\bullet}$ is the dominator because of the solution pH dropping to an acid state as the reaction proceeds. However, the •OH may also participate in the BPA oxidation in the 2nd-stage of the process.

Though thermal and UV activations are two of the ways to control the generation of $SO_4^{-\bullet}$, as described in Eq. (3), many transition metals, especially divalent metals (Mn^{2+}) which are commonly seen and are important in soil and groundwater systems, may act as electron donors to catalyze the decomposition of persulfate through an one-electron transfer reaction analogous to the Fenton initiation reaction. Initiation reactions of Fe^{2+} result in the formation of sulfate radicals [26,27]:

$$Fe^{2+} + S_2O_8^{2-} \rightarrow SO_4^{-\bullet} + SO_4^{2-} + Fe^{3+} \quad (5)$$

$$Fe^{2+} + SO_4^{-\bullet} \rightarrow SO_4^{2-} + Fe^{3+} \quad (6)$$

Fig. 4 shows the comparative study (pH, $[BPA]/[BPA]_0$, and sulfate generation) of the two-stage oxidation process including

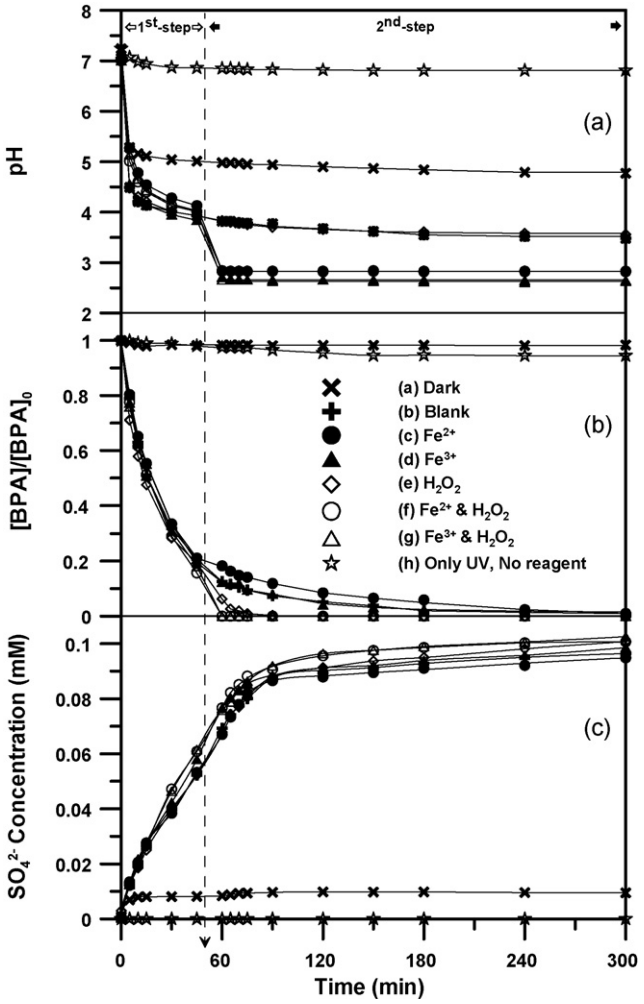

Fig. 4. The pH variations of reaction solutions including the 1st-stage oxidations and the 2nd-stage oxidations (from $t = 50$ min, pH < 4) (a); BPA degradation during various two-stage oxidations (b) and the sulfate ions generation during various two-stage oxidations (c). The 1st-stage shows the presence of $Na_2S_2O_8$ (a); UV + $Na_2S_2O_8$ (b–g); the 2nd-stage is the additional additives of Fe^{2+} (c); Fe^{3+} (d); H_2O_2 (e); $Fe^{2+} + H_2O_2$ (f) and $Fe^{3+} + H_2O_2$ (g). The comparative background experiment for the single photodegradation of BPA with no reagent (h). $[BPA]_i = 0.05$ mM, $[SPS]_i = 0.05$ mM, $[Fe(II,III)]_i = 0.045$ mM, and $[H_2O_2]_i = 0.1579$ mM. Reaction temperature = 25 °C.

extra Fe(II,III) activation, H_2O_2 promotion, and Fe(II,III)/H_2O_2 promotions. Consequently, high mineralization performances can be found in Table 1, corresponding to the tendency of 2nd-stage processes displayed in Fig. 4(b). In comparison, the single use of the $S_2O_8^{2-}$ process can reach the efficacy of total decomposition of BPA, but very rarely for TOC removal. The additional additive of H_2O_2 (or Fe(II,III)) can contribute to a ~25% TOC removal (or 25–34% TOC removal). This is due to the additional •OH donated by additional UV/H_2O_2 processes, or the additional activator (Fe(II,III)) for decomposing remaining persulfate to $SO_4^{-\bullet}$ more completely as in the 2nd-stage processes. 87–91% of high TOC removal is achieved in the Fe(II,III)/H_2O_2 promoted 2nd-stage process used to ensure the detoxication of BPA: it indicates that the photo-Fenton (UV/Fe(II,III)/H_2O_2) can proceed successfully from pH_i 7 by the combination of the $S_2O_8^{2-}$ process. The concentration of SO_4^{2-} produced in each process reached almost the same terminal amounts (~0.1 mM) after around 2 h, which conformed to the stoichoimetric ratio from the theoretical decomposition of 0.05 mM $S_2O_8^{2-}$ (Fig. 4(c)).

Table 1
Comparison of TOC removals between various 2nd-step complex oxidation processes

Run	UV oxidation steps: a + b	TOC removal (%)					
		1st-step: $Na_2S_2O_8$[a] (reaction time (min))		2nd-step: additives adding[b] (reaction time (min))			
	b:	0	45	50	65	90	300
1	Non (blank)	0	1	1	1	1	1
2	H_2O_2	0	1	17	20	20	25
3	Fe^{2+}	0	1	8	18	22	25
4	Fe^{3+}	0	1	31	33	34	34
5	$Fe^{2+} + H_2O_2$	0	1	45	79	85	91
6	$Fe^{3+} + H_2O_2$	0	1	30	66	72	87

[a] The 1st-steps are present of UV + $Na_2S_2O_8$ (runs 1–6)
[b] The 2nd-steps are additional reagents of nothing (run 1), H_2O_2 (run 2), Fe^{2+} (run 3), Fe^{3+} (run 4), $Fe^{2+} + H_2O_2$ (run 5), and $Fe^{3+} + H_2O_2$ (run 6)

In addition, •OH is generated during the persulfate propagation reaction (Eq. (2)). Sulfate radicals and hydroxyl radicals are strong oxidants that can potentially oxidize many common contaminants [14]. But unlike the non-specific oxidation ability of hydroxyl radicals, sulfate radicals act as a relatively selective oxidant that reacts with certain organic compounds [28,29], especially benzene derivatives with ring activating groups [30].

3.3. Thermal effect and kinetics approach

The decomposition of persulfate in aqueous solution is an important step in producing powerful sulfate radicals which destroy organic compounds such as BPA. However, Liang et al. [15,31] suggested that it requires a relatively high activation energy of around 108–130 kJ mol^{-1}, and that the reaction is relatively slow at room temperature for trichloroethylene (TCE) degradation. Thus, temperature is an important factor influencing the decomposition of persulfate and the generation of $SO_4^{-\bullet}$ radicals.

A kinetic study was first suggested by Kolthoff and Miller [32] which showed that the $S_2O_8^{2-}$ decomposition rate at any pH can be expressed by the first-order reaction rate and is catalyzed by hydrogen ions. Some studies have also approached the kinetics of the TCE oxidation reaction with persulfate [11,23,31].

Based on this, the effects of temperature and the activation energy of our BPA degradation system were then studied. Fig. 5 shows the influence of temperature on persulfate oxidation of BPA over a range of 25–50 °C. BPA degradation rates can be improved under thermally enhanced conditions resulting in the degradation of BPA after 1 h being ~88% at 25 °C, ~96% at 35 °C, and ~99% at 50 °C, respectively.

Accordingly, it was found in this BPA/UV/$S_2O_8^{2-}$ process that the BPA degradation is also well formulated to the pseudo-first-order kinetics suggested by some research groups [11,23,25,31]. There is a very good fit of all the experimental data to a pseudo-first-order model (R^2 = 0.99), using the exponential regression analysis (data presented in Table 2) formulated from the original plot of the normalized remaining concentration ([BPA]/[BPA]$_0$) vs. reaction time (t) (Fig. 5). The pseudo-first-order rate constants (k_{obs}) of BPA degradation were found to be 0.038 min^{-1} (R^2 = 0.99) at 25 °C, 0.057 min^{-1} (R^2 = 0.99) at 35 °C, and 0.087 min^{-1} (R^2 = 0.99) at 50 °C, respectively, which increased with increased temperatures.

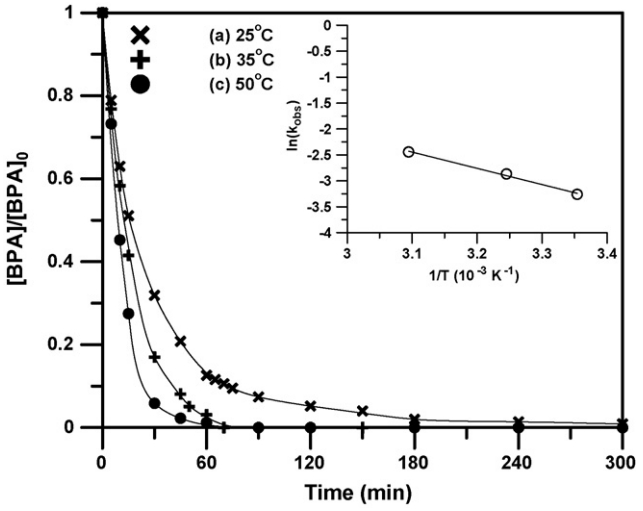

Fig. 5. Effects of temperature (25–50 °C) on BPA degradation by the thermal decomposition of $Na_2S_2O_8$ (a). [BPA]$_i$ = 0.05 mM, [SPS]$_i$ = 0.05 mM. Inserted figure: Arrhenius plot for BPA degradation. The data points used for determining k_{obs} values and ΔE are within the reaction time = 60 min.

The activation energy of the thermal crack of the O–O bond of $S_2O_8^{2-}$ (Eq. (3)) was also reported to be 140.2 kJ mol^{-1} by Kolthoff and Miller [32]. In comparison to Table 2, the activation energy (ΔE = 26 kJ mol^{-1}) in this UV/persulfate system is well estimated from the Arrhenius plot (inserted figure in Fig. 5) and is much lower than that reported by these researchers [11,15,31,32]. This may be due to the structure of different organic target compounds and the shrinkage of the reaction energy barrier (Eq. (3)) by extra activation from a UV source (254 nm).

Table 2
The rate constants of BPA decomposition in UV/persulfate process as a function of temperature

Temperature (K)	[BPA]$_0$ (mM)	[$S_2O_8^{2-}$]$_0$/[BPA]$_0$	$k_{obs} \times 10^2$ (min^{-1})[a]	R^2 of k	$t_{1/2}$ (min)[b]	ΔE (kJ mol^{-1})	R^2 of ΔE
298	0.05	1	3.80 ± 0.04	0.99	16	25.99	0.99
308	0.05	1	5.60 ± 0.09	0.99	12		
323	0.05	1	8.70 ± 0.09	0.99	9		

[a] The observed rate constants were approached to simulate the oxidation of BPA by UV/persulfate according to the pseudo-first-order kinetics suggested by Liang et al. [31] and Huang et al. [25].
[b] Half-life time of BPA in UV/persulfate oxidation process.

4. Conclusions

Sodium persulfate is a potential alternative oxidant for extensive use because of its high water solubility and stability at the ambient temperature (25 °C), and because sulfate ions are relatively harmless and environmentally friendly which are the major products resulting from the reduction of persulfate.

Only a minimum molar ratio of $[S_2O_8{}^{2-}]_0/[BPA]_0 = 1$ is required from the neutral pH_i condition to promote the traditional Fenton's reagents ($[Fe(II,III)]_0/[H_2O_2]_0 < 1$, and a ThOD of $[H_2O_2]_0/[BPA]_0$) utilized during the proposed 2nd-stage oxidation process as pH < 4. Hence, the proposed procedure has great potential and can be practically implemented in industry. As the successful results show, very high removals of TOC (~90%) resulting in BPA detoxication were achieved to improve not only the worse mineralization of single persulfate oxidation, but also to overcome the drawback of traditional Fenton's reagents ($pH_i < 4$).

Acknowledgements

The authors would like to thank the National Science Council of the Republic of China, Taiwan, for financially supporting this research under contract no. NSC 96-2221-E-006-022.

References

[1] C.A. Staples, P.B. Dorn, G.M. Klecka, S.T. O'Block, L.R. Harris, A review of the environmental fate, effects, and exposures of bisphenol A, Chemosphere 36 (1998) 2149–2173.
[2] C.A. Staples, P.B. Dorn, G.M. Klecka, S.T. O'Block, D.R. Branson, L.R. Harris, Bisphenol A concentrations in receiving waters near US manufacturing and processing facilities, Chemosphere 40 (2000) 521–525.
[3] T.E. Schafer, C.A. Lapp, C.M. Hanes, J.B. Lewis, J.C. Wataha, G.S. Schuster, Estrogenicity of bisphenol A and bisphenol A dimethacrylate in vitro, J. Biomed. Mater. Res. 45 (1999) 192–197.
[4] T. Hirano, Y. Honda, T. Watanabe, M. Kuwahara, Degradation of bisphenol A by the lignin-degrading enzyme, manganese peroxidase, produced by the white-rot basidiomycete, *Pleurotus ostreatus*, Biosci. Biotech. Biochem. 64 (2000) 1958–1962.
[5] Y. Tsutsumi, T. Haneda, T. Nishida, Removal of estrogenic activities of bisphenol A and nonylphenol by oxidative enzymes from lignin-degrading basidiomycetes, Chemosphere 42 (2001) 271–276.
[6] Y.H. Huang, Y.F. Huang, P.S. Chang, C.Y. Chen, Comparative study of oxidation of dye-Reactive Black B by different advanced oxidation processes: Fenton, electro-Fenton and photo-Fenton, J. Hazard. Mater. 154 (2008) 655–662.
[7] Y.H. Huang, S.T. Tsai, Y.F. Huang, C.Y. Chen, Degradation of commercial azo dye reactive Black B in photo/ferrioxalate system, J. Hazard. Mater. 140 (2007) 382–388.
[8] S. Tanaka, M. Kawai, Y. Nakata, M. Terashima, H. Kuramitz, M. Fukushima, Degradation of bisphenol A by photo-Fenton processes, Toxicol. Environ. Chem. 85 (2003) 95–102.
[9] W.M. Latimer, Oxidation Potentials, Prentice-Hall, Inc., Englewood Cliffs, NJ, 1952.
[10] L. Eberson, Electron Transfer Reactions in Organic Chemistry, Spring-Verlag, Berlin, 1987.
[11] C.J. Liang, I.L. Lee, I.Y. Hsu, C.P. Liang, Y.L. Lin, Persulfate oxidation of trichloroethylene with and without iron activation in porous media, Chemosphere 70 (2008) 426–435.
[12] E. Hayon, A. Treinin, J. Wilf, Electronic spectra, photochemistry, and autoxidation mechanism of the sulfite–bisulfite–pyrosulfite systems. SO^{2-}, SO^{3-}, SO^{4-}, and SO^{5-} radicals, J. Am. Chem. Soc. 94 (1972) 47–57.
[13] G.R. Peyton, The free-radical chemistry of persulfate-based total organic carbon analyzers, Mar. Chem. 41 (1993) 91–103.
[14] K.C. Huang, Z.Q. Zhao, G.E. Hoag, A. Dahmani, P.A. Block, Degradation of volatile organic compounds with thermally activated persulfate oxidation, Chemosphere 61 (2005) 551–560.
[15] C.J. Liang, Z.S. Wang, C.J. Bruell, Influence of pH on persulfate oxidation of TCE at ambient temperatures, Chemosphere 66 (2007) 106–113.
[16] X.Y. Yu, Z.C. Bao, J.R. Barker, Free radical reactions involving Cl^-, $Cl_2{}^-$, and $SO_4{}^-$ in the 248 nm photolysis of aqueous solutions containing $S_2O_8{}^{2-}$ and Cl^-, J. Phys. Chem. A 108 (2004) 295–308.
[17] G.M. Eisenberg, Colorimetric determination of hydrogen peroxide, Ind. Eng. Chem. Anal. Ed. 15 (1943) 327–328.
[18] H. Tamura, K. Goto, T. Yotsuyanagi, M. Nagayama, Spectrophotometric determination of iron(III) with 1,10-phenanthroline in the presence of large amounts of iron(III), Talanta 21 (1974) 314–318.
[19] H. Hori, A. Yamamoto, E. Hayakawa, S. Taniyasu, N. Yamashita, S. Kutsuna, H. Kiatagawa, R. Arakawa, Efficient decomposition of environmentally persistent perfluorocarboxylic acids by use of persulfate as a photochemical oxidant, Environ. Sci. Technol. 39 (2005) 2383–2388.
[20] L. Dogliotti, E. Hayon, Flash photolysis of persulfateions in aqueous solutions. Study of the sulfate and ozonide radical anions, J. Phys. Chem. 71 (1967) 2511–2516.
[21] S.C. Hsu, T.M. Don, W.Y. Chiu, Free radical degradation of chitosan with potassium persulfate, Polym. Degrad. Stabil. 75 (2002) 73–83.
[22] Y. Huang, J. Li, W. Ma, M. Cheng, J. Zhao, J.C. Yu, Efficient H_2O_2 oxidation of organic pollutants catalyzed by supported iron sulfophenylporphyrin under visible light irradiation, J. Phys. Chem. B 108 (2004) 7263–7270.
[23] P.D. Goulden, D.H.J. Anthony, Kinetics of uncatalyzed peroxydisulfate oxidation of organic material in fresh water, Anal. Chem. 50 (1978) 953–958.
[24] J.O. Edwards, Thermal decomposition of peroxodisulphate ions, Rev. Inorg. Chem. 2 (1980) 179–206.
[25] K.C. Huang, R.A. Couttenye, G.E. Hoag, Kinetics of heat-assisted persulfate oxidation of methyl *tert*-butyl ether (MTBE), Chemosphere 49 (2002) 413–420.
[26] G.P. Anipsitakis, D.D. Dionysiou, Transition metal/UV-based advanced oxidation technologies for water decontamination, Appl. Catal. B: Environ. 54 (2004) 155–163.
[27] W.R. Haag, C.C.D. Yao, Rate constants for reaction of hydroxyl radicals with several drinking water contaminants, Environ. Sci. Technol. 26 (1992) 1005–1013.
[28] C. Cuypers, T. Grotenhuis, K.G.J. Nierop, E.M. Franco, A.D. Jager, W. Rulkens, Amorphous and condensed organic matter domains: the effect of persulfate oxidation on the composition of soil/sediment organic matter, Chemosphere 48 (2002) 919–931.
[29] G.H. Scott, E.P. Bruce, In-Situ Chemical Oxidation-Engineering Issue, Ground Water and Ecosystem Restoration Information Center, UAEPA, EPA/600/R-06/072, 2006, http://www.epa.gov/ada/download/issue/600R06072.pdf.
[30] P. Neta, V. Madhavan, H. Zemel, R.W. Fessenden, Rate constants and mechanism of reaction of sulfate radical anion with aromatic compounds, J. Am. Chem. Soc. 99 (1977) 163–164.
[31] C.J. Liang, C.J. Bruell, M.C. Marley, K.L. Sperry, Thermally activated persulfate oxidation of trichloroethylene (TCE) and 1,1,1-trichloroethane (TCA) in aqueous systems and soil slurries, Soil Sediment Contam. 12 (2003) 207–228.
[32] I.M. Kolthoff, I.K. Miller, The chemistry of persulfate. I. The kinetics and mechanism of the decomposition of the persulfate ion in aqueous medium, J. Am. Chem. Soc. 73 (1951) 3055–3059.